Journal of Science and Engineering Technology, Vol. 3, No. 1, pp. 69-75 (2007)

The Effects of Cutoff Voltage and Heat Treatment on the Behavior of a Nanocrystalline Cu-Doped Tin Oxide Applied to a Li-Ion Battery

SHAO-TING CHANG[1], ING-CHI LEU[2] and MIN-HSIUNG HON[1]

[1] *Department of Materials Science and Engineering, National Cheng Kung University, 1 Ta-Hsueh Rd., Tainan, Taiwan*

[2] *Department of Materials Science and Engineering, National United University No. 1, Lien Da, Kung-Ching Li, Miao-Li, Taiwan*

ABSTRACT

A nanocrystalline Cu-doped tin oxide (5 nm) coating was obtained by electrodeposition in a nitrate solution with Cu as the substrate. The effects of the cutoff voltage range and heat treatment on the electrochemical behaviors of an electrodeposited SnO_2 coating were examined. In a long-term test, both the decomposition of Li_2O during the charging stage in the high-voltage range and the consumption of the electrolyte in the low-voltage range (0 – 0.3 V vs. Li/Li^+) damaged the electrochemical behavior of the Cu-doped tin oxide. The grain refinement during the discharging stage, caused by the transformation from Cu-doped SnO_2 to metallic Sn and Cu, kept the grain size of the metallic particles at around 3 nm. This refinement avoided the capacity fading resulting from the grain growth of tin particles. Moreover, the heat treatment at 400^o C enhanced the cyclability, due to the elimination of an OH bond and adsorbed H_2O molecules, where less Li_2O formed during the first discharging stage reduced the electric resistivity compared with the as-deposited coating. In the case of 1.5 V - 0.3 V, both a high capacity and good cycling were obtained due to the capacity contribution from the reaction of Li_2O and good adhesion between the active particles and the Li_2O matrix.

Key Words: Cu-doped SnO_2, Li-ion batteries, heat treatment, cutoff voltage range, lithium oxide, anode

充放電電壓區間與熱處理對銅摻雜氧化錫奈米晶於鋰離子電池應用之影響

張韶廷[1]　呂英治[2]　洪敏雄[1]

[1] 成功大學材料科學及工程學系

台南市大學路 1 號

[2] 聯合大學材料科學工程學系

苗栗市恭敬里聯大 1 號

摘 要

以電化學沈積法在硝酸溶液中，銅摻雜氧化錫（Cu-doped tin oxide）奈米晶粒（5nm）鍍膜已成功被沈積於銅基板上。充放電電壓範圍與熱處理條件對其電化學性質之影響在本文中將進行深入探討。在長時間測試中，在充電過程於高電壓區間發生之 Li_2O 分解與在低電壓區間（0-0.3V vs. Li/Li^+）發生之電解質消耗均會降低銅摻雜氧化錫奈米晶粒之電化學性質。在放電過程中銅摻雜氧化錫轉變爲金屬錫與銅所造成的晶粒細化，使得金屬粒子的尺寸大小維持在大約 3nm 左右。此一晶粒細化的過程避免了由於錫粒子晶粒成長所造成的電容量下降。與初鍍膜相比，經過 400°C 熱處理的薄膜，由於在表面所吸附的 OH 鍵與 H_2O 分子較少，使得在第一次放電過程中產生較少電子導電性差的 Li_2O，進而提升了其循環性。在 1.5V-0.3V 的充放電電壓範圍，由於 Li_2O 的反應性及 Li_2O 與活性粒子間的良好附著性，而可以同時得到優異的循環性與高的電容量。

關鍵詞：銅摻雜氧化錫，鋰離子電池，熱處理，充放電電壓區間，氧化鋰，陽極

I. INTRODUCTION

In recent years, lithium-ion batteries are becoming the main power sources of rechargeable batteries for portable electronics [1, 10, 13, 14, 16, 22]. They can store more energy per unit volume or weight than that of nickel-metal hydride, nickel-cadmium and lead-acid batteries. Although graphite is available commercially as an anode material for Li-ion battery, the research of high-performance materials is still an active area.

Nanocrystalline and Cu-doped SnO_2 can be obtained by electrodeposition with Cu as substrate, which is a fast, low-cost, low temperature, and convenient process [3]. Furthermore, the electrodeposited tin oxide coating reveals the stable electrochemical behaviors since the coating does not contain any binder or carbon black, which could influence the capacity and cyclability. The as-deposited coating can be employed to analyze its behavior directly without any extra procedure to damage its property. In the previous paper [3], the reactions during change/discharge have been studied, and found that a Li_2O matrix forms and surrounds the metallic particles, nano-sized Sn and Cu particles in the discharge step of the first cycle.

$$Sn_{1-x}Cu_xO_{2-x} + (4-2x)Li^+ + (4-2x)e^- \rightarrow (1-x)Sn + xCu + (2-x)Li_2O \quad (1)$$

The nano-sized Cu particles are formed during the discharge step, as well as nano-sized Sn particles. The x denotes the ratio of Cu to Sn in the Cu-doped SnO_2 lattice, in between 0.03 to 0.25 from the chemical composition analysis. In the lower voltage range, the dominant reaction is the formation/decomposition of Sn-Li alloy, as described by the following reaction [3-4].

$$4.4Li^+ + Sn + 4.4e^- \rightarrow Li_{4.4}Sn \quad (2)$$

We also found that the Li_2O matrix, supposed to be an electrochemically inert material [17], is activated in a high voltage range (around 1.2V vs. Li^+/Li) in the charge step. Both the Cu-doping in SnO_2 lattice and the nanosized SnO_2 particles activate the Li_2O if the anode is free from binder and carbon black.

$$3Li_2O + Cu + Sn \leftrightarrow CuO + SnO_2 + 6Li^+ + 6e^- \quad (3)$$

Although the reaction involved Li_2O enhances the capacity, the decomposition of Li_2O weakens the adhesion between the active particles and Li_2O matrix, which damages the cyclability. Thus, the conditions of charge/discharge have to be carefully selected to obtain an optimum electrochemical property.

Because cracks are formed in both high voltage range (above 1.5 V) and low voltage range (around 0 V), the choice of cutoff voltage range significantly affects the electrochemical behavior. Thus, the effects of heat treatment and different cutoff voltage ranges on the electrochemical behaviors for Li-ions battery are investigated. FT-IR spectrum is employed to observe the structure change after heat treatment. These results are described and correlated with the reaction during charge and discharge for 50 cycles.

II. EXPERIMENT

The preparation of nanocrystalline SnO_2 coating was reported in the previous paper [3], in which some of the samples were heat-treated at 400 ^oC in a vacuum atmosphere

for 4 hr to remove the OH bond and absorbed H_2O molecules in SnO_2. The high vacuum inhibited the oxidation reaction on the copper surface and no debris was found on the coating after heat treatment. Both the heat-treated and as-deposited samples were compared to study the electrochemical behaviors for Li-ions battery, which were carried out in a traditional coin-cell, using lithium sheets as the counter electrode. The electrolyte used was 1 M anhydrous $LiPF_6$ in an 1:1 mixture of ethylene carbonate and dimethyl carbonate. Only four to five drops of electrolyte (around 0.25 ml) were sealed in the cell and the sealing procedure was conducted in the glove box filled with Ar gas. These cells were cycled at a current density of 100 mA g^{-1} through different ranges of voltage, controlled via Arbin BT2043. Several cutoff voltage ranges were used to optimize the properties of electrodeposited SnO_2 coating for Li-ion battery. The maximum and minimum voltages ranged from 2.5 V to 1.0 V and 0.3 V to 0.05V vs. Li^+/Li respectively were used.

In the previous studies, it was found that nano-crystalline Li_2O was decomposed in the charge step, as observed in the differential capacity vs. voltage diagram. The capacity of Li_2O formation/decomposition was calculated by the area under the reaction peak around 1.2 V vs. Li^+/Li. The difference between the heat-treated and as-deposited SnO_2 coating was analyzed by the FT-IR spectrum, performed on a Jasco FT-IR 460 spectrometer.

III. RESULTS AND DISCUSSION

1. The Effect of Cutoff Range

Figure 1 shows the capacity of the as-deposited SnO_2 in the different cutoff voltage ranges. The capacities for the maximum cutoff voltage of 2.5 V, 1.5 V, and 1.0 V for 50 cycles are shown in Figure 1 (a), (b), and (c) respectively. The cases of 2.5 V to 0.05 V were measured only up to 47 cycles, as limited by the memory capacity of the computer. A higher maximum voltage (2.5 V and 1.5 V) results in a poor cyclability, due to the serious decomposition of Li_2O in a higher voltage range (around 1.2 V) during the charge step [3, 24]. Li_2O functions as glue here [24] for active particles and thus the decomposition damages the adhesion between active particles and Li_2O matrix, causing the reduce of the cyclability. Thus, a higher maximum voltage leads to a higher capacity in the beginning, but the capacity decreases drastically in the subsequent cycles. Raising the minimum cutoff voltage to 0.3 V from 0.05 V promotes the cyclability, as observed by the previous researchers [5, 19], which was performed by inhibiting the severe volume change of Sn-Li alloy at the voltage range more negative than 0.3 V. The cutoff voltage

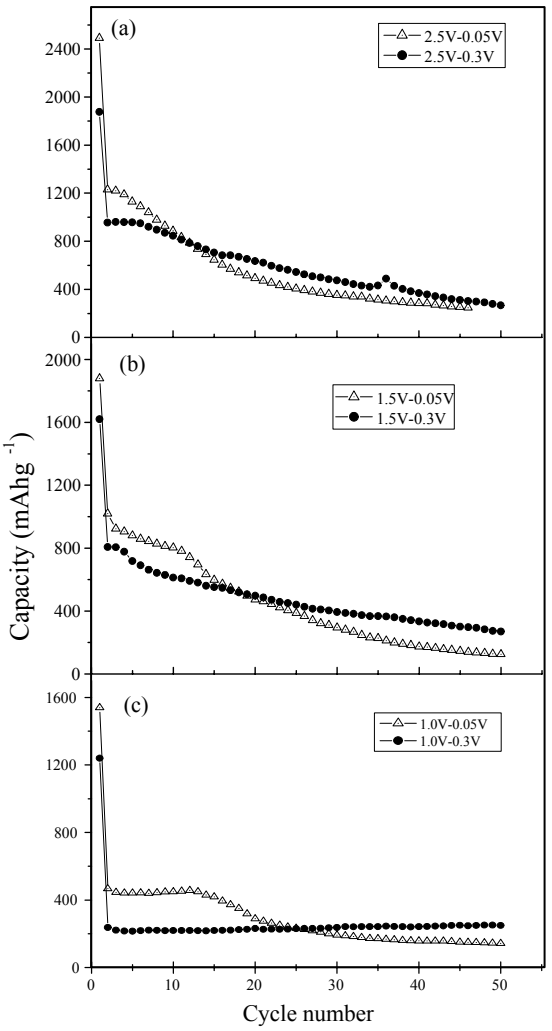

Fig. 1. Discharge capacities of the as-deposited Cu-doped tin oxide coatings for the maximum cutoff voltages of (a) 2.5 V, (b) 1.5 V, and (c) 1.0 V

range of 1.0 V to 0.05 V, thus, offers an extreme cyclability, almost keeping at a constant value (220 mAh g^{-1}) after the second cycle.

Some data in these figures are still very important in spite of that the electrochemical behaviors of the as-deposited SnO_2 coating are not satisfied. First, it is very obvious that the capacity differences between the minimum voltages of 0.05 V and 0.3 V in Figure 1 are around 200 mAh g^{-1} in first several cycles, which can be attributed to the formation of $Li_{4.4}Sn$ and the reaction of electrolyte. The nano-sized Cu particles, precipitated from the Cu-doped SnO_2 lattice, catalyze the electrolyte in the low voltage range [7], and thus the limit electrolyte (0.25 ml) in the cell is consumed. The electrolyte runs out after a few cycles resulting in a sudden drop for the minimum voltage of 0.05 V in Figure 1 (b) and (c). In the test with a capacity drop, white crystals can be found between work

and counter electrodes as the cell is taken apart in an Ar-filled glove box. The crystal also improves the consuming electrolyte. The capacity drop in Figure 1(a) is not so obvious because the capacity loss from Li_2O decomposition is larger than that from consuming electrolyte.

Figure 2 shows the percentages of the discharge capacities from the reaction of Li_2O for different cutoff voltage ranges. The capacity contribution from the reaction involving Li_2O decomposition shown is calculated by the area under the reaction peak [3]. For the cutoff voltage range of 2.5 V to 0.05 V, the discharge capacity of Li_2O contribution decreases in the first fifteenth cycles and then maintains a constant value of about 10%, while that for 1.5 V to 0.05 V keeps declining. The decrease of Li_2O contribution might be attributed to the aggregation of metallic Sn [6] and the formation of crack during charge and discharge, which lead to the decrease of contact area between active metallic particles and Li_2O matrix. Because the formation of crack does not affect the percentage of Li_2O contribution, the possible reason involving cracks formation can be eliminated here. Moreover, the grain growth of metallic Sn particles after numerous cycles was observed by previous researchers [25]. The growth not only causes the decay of the electrochemical behavior, but also reduces the activity of the metallic Sn particle and consequently might result in the decrease of the Li_2O contribution. The TEM analysis will monitor the grain growth during charge/discharge.

The TEM bright image in our previous paper indicated that the grain size of the as-deposited coating was around 5 nm. Figure 3 (a) shows the TEM bright image of sample ended at 0.7 V vs. Li/Li^+ in the first discharge step, which reveals that the average particle size of electrodeposited SnO_2 is about 2-3 nm. Figures 3 (b) and (c) show the bright images of the coatings after 50 cycles discharge and charge, where the sample

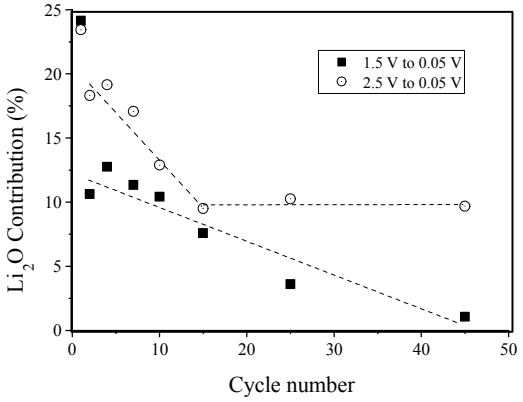

Fig. 2. Percentages of the discharge capacity from the reaction of Li_2O for the cutoff voltage ranges of 2.5 – 0.05 V and 1.5 – 0.05 V

in Figure 3(b) is ended at 0.7 V and that in Figure 3(c) is 2.5 V. Each of these two is held at the terminal voltage for 1 hr to highlight the reaction at its respective voltage. The grain size in Figure 3 (b) is about 2-3 nm, similar with that of the as-deposited coating. The grain growth of metallic Sn is not observed in the discharge step, while a large grain growth (10 ~ 30 nm) is observed in the sample as ended at 2.5 V in the charge step, as shown in Figure 3 (c). Figure 3 (d) shows the diffraction pattern of the particles in Figure 3(d), and only the diffraction rings of SnO_2 are found. The EDS analysis shows that an obvious amount of Cu species still exists in the sample. It can be concluded that the Cu-doped SnO_2 is formed from ultra-fine Cu and Sn particles in the high voltage range during the charge step with a large grain growth. In the subsequent cycle, the metallic composite of Cu and Sn forms during the discharge step and particles are refined back to 2-3 nm again. As we know, the multi-phase precipitation from single phase can refine the grain size [8, 15, 26]. The formation processing of Cu/Sn composite is similar with the grain refinement caused by the phase transformation. We can conclude that the Cu-doping in SnO_2 inhibits the grain growth, and thus improves its electrochemical behavior.

2. The Effect of Heat Treatment

The heat treatment for the electrodeposited Cu-doped SnO_2 is embarked due to the enhancement of the electro-

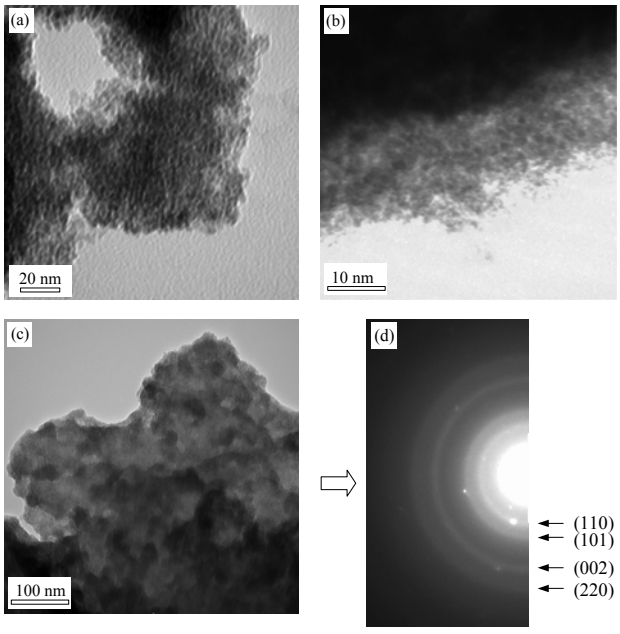

Fig. 3. TEM bright images of the samples as ended at (a) 0.7 V vs. Li/Li^+ in the first discharge, (b) 0.7 V in the 50th discharge step, (c) 2.5 V in the 50th charge step, and (d) its diffraction pattern

chemical behavior of SnO_2 for Li-ion battery [12, 21, 27]. The temperature must be chosen carefully to prevent the grain growth during the heat treatment. The temperature of 400 ^oC removes not only the physically and chemically absorbed H_2O molecules [23] but also the hydroxide bonded in SnO_2 [9], while the temperature is also below the one causing grain growth for both un-doped and Cu-doped SnO_2 [29]. In our previous study [2], either impurity or transformation of structure was found after heat treatment at 400 ^oC in vacuum but a better crystallinity was obtained. Figure 4 shows the FT-IR adsorption spectra of the as-deposited and heat-treated SnO_2 coating. It is commonly reported that the IR spectrum of SnO_2 presents a broad band in the range of 400 - 800 cm^{-1} due to the superposition of different vibration modes [9, 28]. The peak located at 1380 cm^{-1} can be assigned to the binary combination of the band of SnO_2 at 650 cm^{-1} and thus can be attributed to the vibration modes of the bridged species Sn-O-Sn. Meanwhile, the signals of copper oxide (including CuO and Cu_2O) located in the range of 500 – 800 cm^{-1} [11], are highly overlapping with SnO_2. Thus, the absorbed spectra of tin oxide and cooper oxide combine into a broader peak, which are difficult to be distinguished. An obvious difference between these two spectra is the significant decrease of a broad band located at 3400 cm^{-1}. The broad signal can be attributed to the symmetric (ν_1) and antisymmetric stretching (ν_3) modes of water, locating at 3230 and 3380 cm^{-1}, respectively [18]. The decrease can be concluded that most OH bond and H_2O molecules are eliminated during the heat treatment of 400 ^oC in vacuum. The peak at 1640 cm^{-1}, which can be assigned as the bending mode of H-O-H [20], still appears after heat treatment, which is the evidence of the existence of molecular water and thus it can be concluded that the films prepared by electrodeposition contain lattice water. The residual lattice water explains that the small signal of water still can be found in the spectrum of the heat-treated coating. The FT-IR analysis shows that the heat-treated coating has less oxygen element since the adsorbed water and hydroxide bond have been eliminated.

Figure 5 shows the discharge capacities of the heat-treated samples for different cutoff voltage ranges. Since the voltage more negative than 0.3 V leads to the consumption of electrolyte and the crack of Sn-Li alloy, the minimum voltage of 0.3 V is chosen. As compared with the capacities of as-deposited coating (in figure 1), the capacity of the heat-treated coating is lower in the first several cycles but higher after several cycles, which is due to the less oxygen ion in the heat-treated coating. The formation of Li_2O during the discharge step in the first cycle is shown below.

$$SnO_{2-x}(OH)_{2x} + yCuO + zH_2O + 2(2+x+y+z)Li^+ + (4+2y)e^- \rightarrow Sn + y\,Cu + (2+x+y+z)Li_2O + 2(x+y)H^+ \quad (4)$$

where 2x, y, and z indicate the ratio of Sn-OH bonds, CuO, and absorbed H_2O molecules respectively. The copper oxide also contains some OH bonds, however, the equation does not show the copper hydroxide for simplification. According to the equation, few amount of OH bonds and absorbed H_2O molecules will form less Li_2O in the first cycle. As we know, the conductivity of Li_2O is pretty low so that it obstructs electron transfer. If a lot of Li_2O particles surround these active particles, the electric resistance of the anode will be very high, which will lead to a high internal resistivity of the cell. Once the resistance of the electrode is increased, more power is consumed during charge/discharge, and then degrades the electrochemical performance of the cell. Thus, the amount of

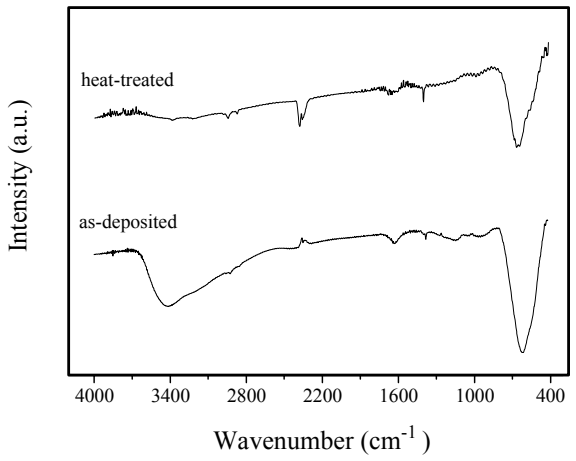

Fig. 4. FT-IR spectra of the as-deposited and heat-treated Cu-doped tin oxide coatings

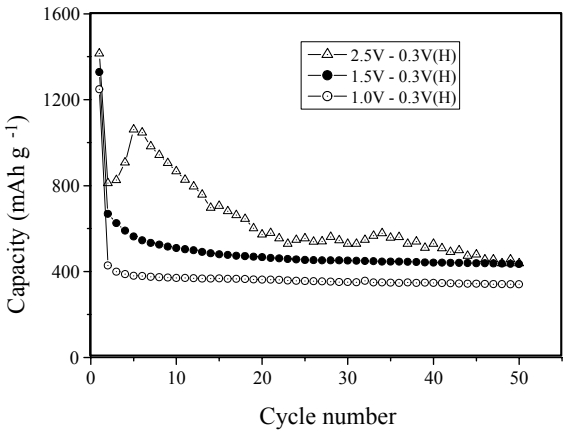

Fig. 5. Discharge capacities of the heat-treated sample for different cutoff voltage ranges

Li_2O formed in the first cycle significantly affects electrochemical behavior of the electrode.

In Figure 5, it is also found that the discharge capacity of 50 cycles for the cutoff voltage range of 2.5 V to 0.3 V decreases to 438 mAh g^{-1} from the second cycle (813 mAh g^{-1}). The poor cycling is due to the formation of cracks by the severe decomposition of Li_2O in the high voltage range (1.5 V ~ 2.5 V) [3]. Meanwhile, the cutoff voltage range of 1.0 V to 0.3 V cannot offer a high enough overpotential and thus its capacity is the lowest one in these three cases, while its cyclability is the best one among them. For the voltage range between 1.5 V and 0.3 V, the capacity contribution from the reaction involving Li_2O is still maintained, however, the decomposition of Li_2O does not weaken the adhesion between active particles and Li_2O matrix. Thus, the voltage range of 1.5 V to 0.3 V of the heat-treated SnO_2 coating possesses not only a high capacity but also a good cyclability, where the capacity for 50th cycle is around 435 mAh g^{-1}, higher than the theoretical capacity of commercial graphite (372 mAh g^{-1}). Although the capacities of the maximum voltages of 2.5 V and 1.5 V are almost the same, the capacity of 1.5 V will be better after 50 cycles because of its superior cyclability

IV. CONCLUSION

The effects of the cutoff voltage range and the heat treatment on the electrochemical behavior of the electrodeposited SnO_2 coating are examined. The Li_2O decomposes seriously during the charge step in high voltage range more positive than 1.5 V so that the adhesion of the active particles and the Li_2O matrix is weakened. For the voltage range more negative than 0.3 V, the electrolyte is being consumed after several cycles because metallic Cu formed during the discharge step. Both of the Li_2O decomposition and the electrolyte consumption damage the electrochemical property of the Cu-doped tin oxide. Thus, the voltage range larger than 1.5 V and the range smaller than 0.3 V should be avoided. During the discharge step, the grain refinement, caused by the transforming from Cu-doped SnO_2 to the mixture of Cu and Sn particles, keeps the grain size of metallic particles around 3 nm rather than grows with cycle number. The stability of grain refinement eliminates the capacity fading in charge/discharge process.

The heat treatment at 400 ^oC in vacuum removes the OH bonds and the absorbed H_2O molecules in the electrodeposited SnO_2 coating. The elimination of "extra oxygen" in coating minimizes the formation of Li_2O and also lessens the internal resistance of the cell. Therefore, the heat treatment enhances the electrochemical performance of the Cu-doped nanocrystalline SnO_2 coating. The voltage range between 1.5 V and 0.3 V for the heat-treated SnO_2 coating not only keeps the capacity contribution from the reaction of Li_2O, but also avoids weakening the adhesion between the active particles and Li_2O matrix. Thus, the heat-treated coating has both a high capacity and a good cycling in the cutoff voltage range mentioned above. After 50 cycles, the capacity is around 435 mAh g^{-1}, higher than that of the commercial graphite electrode.

V. ACKNOWLEDGEMENT

The authors gratefully acknowledge the financial support by the National Science Council of TAIWAN. (NSC92-2120-M -006-003).

REFERENCES

1. Atwater, T. B., P. J. Cygan and F. C. Leung (2000) Man portable power needs of the 21st century: I. Applications for the dismounted soldier. II. Enhanced capabilities through the use of hybrid power sources. *Journal of Power Sources*, 91(1), 27-36.
2. Chang, S. T., I. C. Leu and M. H. Hon (2002) Preparation and characterization of nanostructured tin oxide films by electrochemical deposition. *Electrochemical and Solid-State Letters*, 5(8), C71-74.
3. Chang, S. T., I. C. Leu, C. L. Liao, J. H. Yen and M. H. Hon (2004) Electrochemical behavior of nanocrystalline tin oxide electrodeposited on a Cu substrate for Li-ion batteries. *Journal of Materials Chemistry*, 14(12), 1821-1826.
4. Courtney, I. A. and J. R. Dahn (1997) Electrochemical and *In Situ* X-ray diffraction studies of the reaction of lithium with tin oxide composites. *Journal of the Electrochemical Society*, 144(6), 2045-2052.
5. Courtney, I. A. and J. R. Dahn (1997) Key factors controlling the reversibility of the reaction of lithium with SnO_2 and Sn_2BPO_6 glass. *Journal of the Electrochemical Society*, 144(9), 2943-2948.
6. Courtney, I. A., W. R. Mckinnon and J. R. Dahn (1999) On the aggregation of tin in SnO composite glasses caused by the reversible reaction with lithium. *Journal of the Electrochemical Society*, 146(1), 59-68.
7. De´bart, A., L. Dupont, P. Poizot, J-B. Leriche and J. M. Tarascon (2001) A transmission electron microscopy study of the reactivity mechanism of tailor-made CuO particles toward lithium. *Journal of the Electrochemical Society*, 148(1), A1266-1274.
8. Enderle, R., F. G. Neunhoeffer, M Göbbels, F. A. Müller and P. Greil (2005) Influence of magnesium doping on the phase transformation temperature of β-TCP ceramics examined by Rietveld refinement. *Biomaterials*, 26(17),

3379-3384.

9. Giutini, J. C., W. Granier, J. V. Zanchetta and A. Taha (1990) Sol-gel preparation and transport properties of a tin oxide. *Journal of Materials Science Letters*, 9(12), 1383-1388.
10. Hon, Y. M., H. Y Chung, K. Z. Fung and M. H. Hon (2001) NMR and FT-IR investigation of spinel $LiMn_2O_4$ cathode prepared by the tartaric acid gel process. *Journal of Solid State Chemistry*, 160(2), 368-376.
11. Jagminas, A., G. Niaura, J. Kuzmarskytė and R. Butkienė (2004) Surface-enhanced Raman scattering effect for copper oxygenous compounds array within the alumina template pores synthesized by ac deposition from Cu(II) acetate solution. *Applied Surface Science*, 225(1-4), 302-308.
12. Kim, J. Y., D. E. King, P. N. Kumta and G. E. Blomgren (2000) Chemical synthesis of tin oxide-based materials for li-ion battery anodes influence of process parameters on the electrochemical behavior. *Journal of the Electrochemical Society*, 147(12), 4411-4420.
13. Lee, Y. H., I. C. Leu, S. T. Chang, C. L. Liao and K. Z. Fung (2004) The electrochemical capacities and cycle retention of electrochemically deposited Cu_2O thin film toward lithium. *Electrochimica Acta*, 50(2-3), 553-559.
14. Liao, C. L. and K. Z Fung (2004) Lithium cobalt oxide cathode film prepared by rf sputtering. *Journal of Power Sources*, 128(2), 263-269.
15. Liao, S. C. and J. Colaizzi (2000) Refinement of nanoscale grain structure in bulk titania via a transformation-assisted consolidation (TAC) method. *Journal of the American Ceramic Society*, 83(9), 2163-2169.
16. Lin, S. P., K. Z. Fung, Y. M. Hon and M. H. Hon (2002) Effect of Al addition on formation of layer-structured $LiNiO_2$. *Journal of Solid State Chemistry*, 167(1), 97-106.
17. Liu, W., X. Huang, Z. Wang, H. Li and Li Chen (1998) Studies of stannic oxide as an anode material for lithium-ion batteries. *Journal of the Electrochemical Society*, 145(11), 59-62.
18. Max, J. J., M. Trudel and C. Chapados (1998) Subtraction of the water spectra from the infrared spectrum of saline solutions. *Applied Spectroscopy*, 52(2), 234-239.
19. Mohamedi, M., S. J. Lee, D. Takahashi, M. Nishizawa, T. Itoh and I. Uchida (2001) Amorphous tin oxide films: Preparation and characterization as an anode active material for lithium ion batteries. *Electrochimica Acta*, 46(8), 1161-1168.
20. Moina, C. A. and G. O. Ybarra (2001) Study of passive films formed on Sn in the 7–14 pH range. *Journal of Electroanalytical Chemistry*, 504(2), 175-183.
21. Nam, S. C., C. H. Paik, W. I. Cho, H. S. Chun and Y. S. Yun (1999) Electrochemical characterization of various tin-based oxides as negative electrodes for rechargeable lithium batteries. *Journal of Power Sources*, 84(1), 24-31.
22. Owens, B. B., W. H. Smyrl and J. J. Xu (1999) R&D on lithium batteries in the USA: High-energy electrode materials. *Journal of Power Sources*, 81-82, 150-155.
23. Patel, A., G. Coudurier, N. Essayem and J. C. Védrine (1997) Effect of the addition of Sn to zirconia on the acidic properties of the sulfated mixed oxide. *Journal of the Chemical Society, Faraday Transaction*, 93(2), 347-354.
24. Polzot, P., S. Laruelle, S. Grugeon and J. M. Tarascon (2000) Nano-sized transition-metal oxides as negative-electrode materials for lithium-ion batteries. *Nature*, 407, 496-499.
25. Retoux, R., T. Brousse and D. M. Schleich (1999) High-resolution electron microscopy investigation of capacity fade in SnO_2 electrodes for lithium-ion batteries. *Journal of the Electrochemical Society*, 146(7), 2472-2476.
26. Wang, Y., J. N. Wang, J. Yang and Q. Xia (2001) Grain refinement of a TiAl alloy by heat treatment through near gamma transformation. *Journal of Materials Science*, 36(18), 4465-4468.
27. Wang, Y., J. Y. Lee and B. H. Chen (2003) Microemulsion synthesis of tin oxide-graphite nanocomposites as negative electrode materials for lithium-ion batteries. *Electrochemical and Solid-State Letters*, 6(1), A19-A22.
28. Wardell, J. L. (1995) In handbook of inorganic compounds, 4170. S. L. Philips, Ed. CRC Press, New York.
29. Zhang, G. and M. Liu (2000) Effect of particle size and dopant on properties of SnO_2-based gas sensors. *Sensors and Actuators B*, 69(1), 144-152.

收件：94.12.14　修正：95.03.09　接受：95.09.12